Aggregated Silver Nanoparticles-Based Surface-Enhanced Raman Scattering Enzyme-Linked Immunosorbent Assay for Ultrasensitive Detection of Protein Biomarkers and Small Molecular

ARTICLE *in* ANALYTICAL CHEMISTRY · APRIL 2015

Impact Factor: 5.64 · DOI: 10.1021/acs.analchem.5b01011 · Source: PubMed

9 AUTHORS, INCLUDING:

Yong Tang

Jinan University (Guangzhou, China)

22 PUBLICATIONS **191** CITATIONS

SEE PROFILE

analytical chemistry

Article

pubs.acs.org/ac

Aggregated Silver Nanoparticles Based Surface-Enhanced Raman Scattering Enzyme-Linked Immunosorbent Assay for Ultrasensitive Detection of Protein Biomarkers and Small Molecules

Jiajie Liang,[†,∥] Hongwu Liu,[‡,∥] Caihong Huang,[†,∥] Cuize Yao,[†] Qiangqiang Fu,[†] Xiuqing Li,[†] Donglin Cao,[§] Zhi Luo,*[,‡] and Yong Tang*[,†]

[†]Department of Bioengineering, Guangdong Province Key Laboratory of Molecular Immunology and Antibody Engineering, and [‡]Department of Electronic Engineering, Jinan University, Guangzhou 510632, People's Republic of China

[§]Department of Laboratory Medicine, Guangdong No. 2 Provincial People's Hospital, Guangzhou 510317, People's Republic of China

Supporting Information

ABSTRACT: Lowering the detection limit is critical to the design of bioassays required for medical diagnostics, environmental monitoring, and food safety regulations. The current sensitivity of standard color-based analyte detection limits the further use of enzyme-linked immunosorbent assays (ELISAs) in research and clinical diagnoses. Here, we demonstrate a novel method that uses the Raman signal as the signal-generating system of an ELISA and combines surface-enhanced Raman scattering (SERS) with silver nanoparticles aggregation for ultrasensitive analyte detection. The enzyme label of the ELISA controls the dissolution of Raman reporter-labeled silver nanoparticles through hydrogen peroxide and generates a strong Raman signal when the analyte is present. Using this assay, prostate-specific antigen (PSA) and the adrenal stimulant ractopamine (Rac) were detected in whole serum and urine at the ultralow concentrations of 10^{-9} and 10^{-6} ng/mL, respectively. The methodology proposed here could potentially be applied to other molecules detection as well as PSA and Rac.

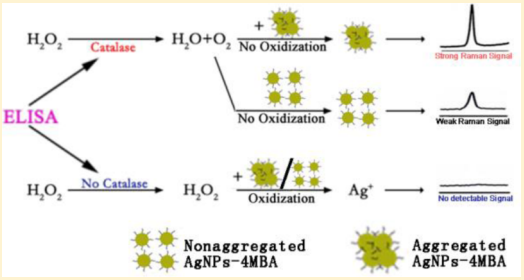

Ultrasensitive detection of protein and small molecular analytes is critical for medical diagnostics, food safety regulations, and environmental monitoring.[1−4] At present, protein and small molecular analytes can be detected by several methods, including enzyme-linked immunosorbent assays (ELISAs),[5] fluorescence-based protein microarrays,[6] electrochemistry,[7] label-free optical methods,[8] surface-enhanced Raman scattering (SERS),[9−11] microcantilevers,[12] and nanotube- or nanowire-based field-effect transistors.[13−15] ELISAs are the most common methods, as they provide accurate, convenient, and robust detection for a large range of applications. Subsequently, many strategies for signal amplification[16,17] and new signifiers are used to increase sensitivity, including fluorescence[18] and chemiluminescence;[19] these strategies can increase detection sensitivity to the picogram range. SERS is also used with an ELISA because of its signal enhancement capability. Commonly, detecting antibodies and Raman reporter molecules are labeled on the surface of nanoparticles, which form the immune Raman probe and exhibit an excellent SERS effect. The antigen concentration can be determined by detecting the Raman signal once the immune Raman probe is combined with the antigen.[20] This combination of the SERS effect and ELISA provides a highly sensitive antigen detection process.

Recently, to improve detection sensitivity, several studies have utilized the reducibility of hydrogen peroxide to alter the metal nanoparticles to allow ultrasensitive detection.[21−25] According to the previous studies,[24,26,27] change of 20 μM hydrogen peroxide can achieve 10^{-18} g/mL ultradetection. Facts proved that such sensors are powerful techniques for chemical and biological sensing experiments.

Here, we introduced aggregated silver nanoparticles (AgNPs)-based SERS into an ELISA signal generation system, termed the aggregated AgNPs-based SERS−ELISA (AAN−SERS−ELISA). Figure 1 schematically depicts the working principle of the signal generation system. Raman reporter (4-mercaptobenzoic acid, 4-MBA) has a characteristic peak of Raman signal at 1077 cm^{-1}, and its Raman signal can be enhanced by coupling it with AgNP.[28] AgNPs can be aggregated by dissolving in saline solution. Because of the greatly enhanced electromagnetic (EM) field produced by the surface plasmon resonance (SPR) on metal nanostructures, particularly in "'hot spots'" of an ensemble of structures, the proper aggregation of AgNPs−4MBA can produce more "hot spots" to increase the intensity of the SERS effect.[28−30] Due to

Received: March 16, 2015
Accepted: April 30, 2015

DOI: 10.1021/acs.analchem.5b01011
Anal. Chem. XXXX, XXX, XXX−XXX

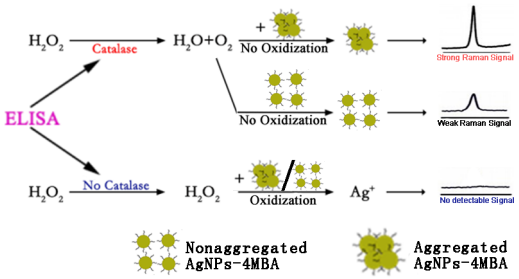

Figure 1. Schematic diagram of silver nanoparticles aggregation based SERS-based signal generation system.

the disappearance or size reduction of AgNPs, the Raman signal of 4-MBA can be reduced by the capability of hydrogen peroxide to oxidize AgNPs to Ag^+. In other words, the detected Raman signal increases as the concentration of hydrogen peroxide reduces. In this paper, we present two general strategies (sandwich and competitive ELISAs) to assess whether the novel signal generation system is viable. Here, we use the sandwich ELISA to illustrate how AAN−SERS−ELISA functions. The procedure of sandwich AAN−SERS−ELISA is shown in Figure 2. As shown in the figure, the operation of AAN−SERS−ELISA is similar to conventional colorimetric ELISA. A large protein biomarker molecule (prostate-specific antigen, PSA) is captured with a specific antibody (capture antibody) on a disposable substrate. Subsequently, the detection probe (detection antibody linked with catalase through gold nanoparticles) is added and combine with PSA. After a full reaction, a certain amount of hydrogen peroxide is added, and if the catalase is in existence, the hydrogen peroxide will be consumed by catalase. That is, the detected Raman signal increases. Therefore, the Raman signal is indirectly proportional to the amount of PSA.

EXPERIMENTAL SECTION

Materials and Chemicals. Silver nitrate ($AgNO_3$, 99.8%) was obtained from Sinoreagent (Shanghai, China). Chloroauric acid ($HAuCl_4$) and Tween-20 were obtained from Amresco. 4-Mercaptobenzoic acid (4-MBA) and bovine serum albumin (BSA) were purchased from Asegene (Guangzhou, China). Catalase (40 000−60 000 units/mg), clenbuterol (Cl), ractopamine (Rac), and PSA were purchased from Sigma-Aldrich. Trisodium citrate was purchased from Damaoreagent (Tianjin, China). Fetal bovine serum was obtained from Life Technology. The 96-well polystyrene plate was purchased from JET BIOFIL. Mouse monoclonal anti-PSA (capture antibody) and secondary antihuman PSA antibody (detection antibody) were obtained from Abcam. The serum samples were collected from the Department of Laboratory Medicine, Guangdong No. 2 Provincial People's Hospital. Hydrogen peroxide (H_2O_2, 30 wt %) and potassium carbonate were purchased from GZ Chemical Reagent (Guangzhou, China). Anti-Rac monoclonal antibodies (mAb) and coating antigen BSA−Rac were produced in our laboratory. Deionized water (Milli-Q grade, Millipore) with a resistivity of 18.2 MΩ·cm was used throughout this study.

Equipment. The absorption spectrum and Raman signal were recorded with a Synergy H1 Hybrid Multi-Mode microplate reader (BioTek) and Advantage 785 Raman spectrometer (DeltaNu). Transmission electron microscopy (TEM) samples were prepared on copper-supported carbon films by depositing a drop of solution and allowing it to dry.

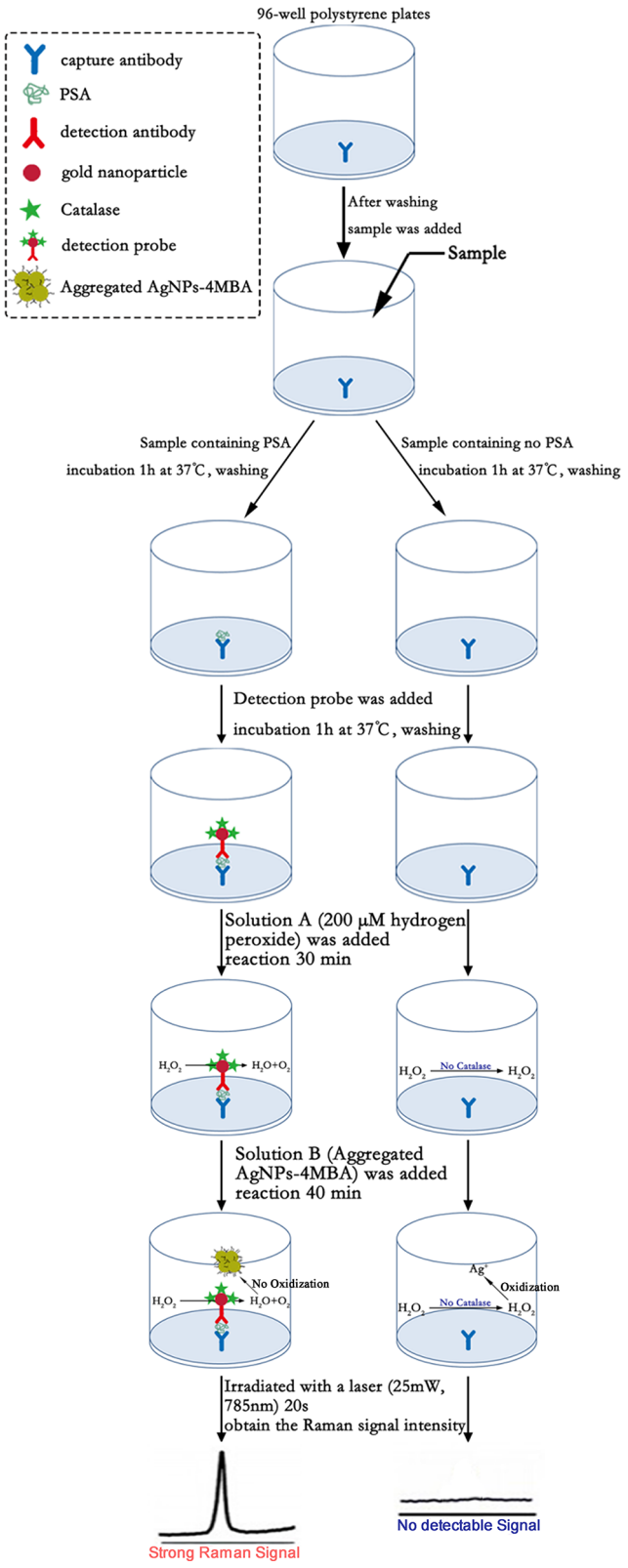

Figure 2. Procedure of aggregated AgNPs-based SERS−ELISA (sandwich format).

TEM images were recorded with a PHILIPS TECNAI-10 transmission electron microscope operating at an acceleration voltage of 120 kV. Dynamic light scattering (DLS), X-ray diffraction (XRD), and inductively coupled plasma mass spectrometer (ICP) data were recorded with a Malvern

DOI: 10.1021/acs.analchem.5b01011
Anal. Chem. XXXX, XXX, XXX−XXX

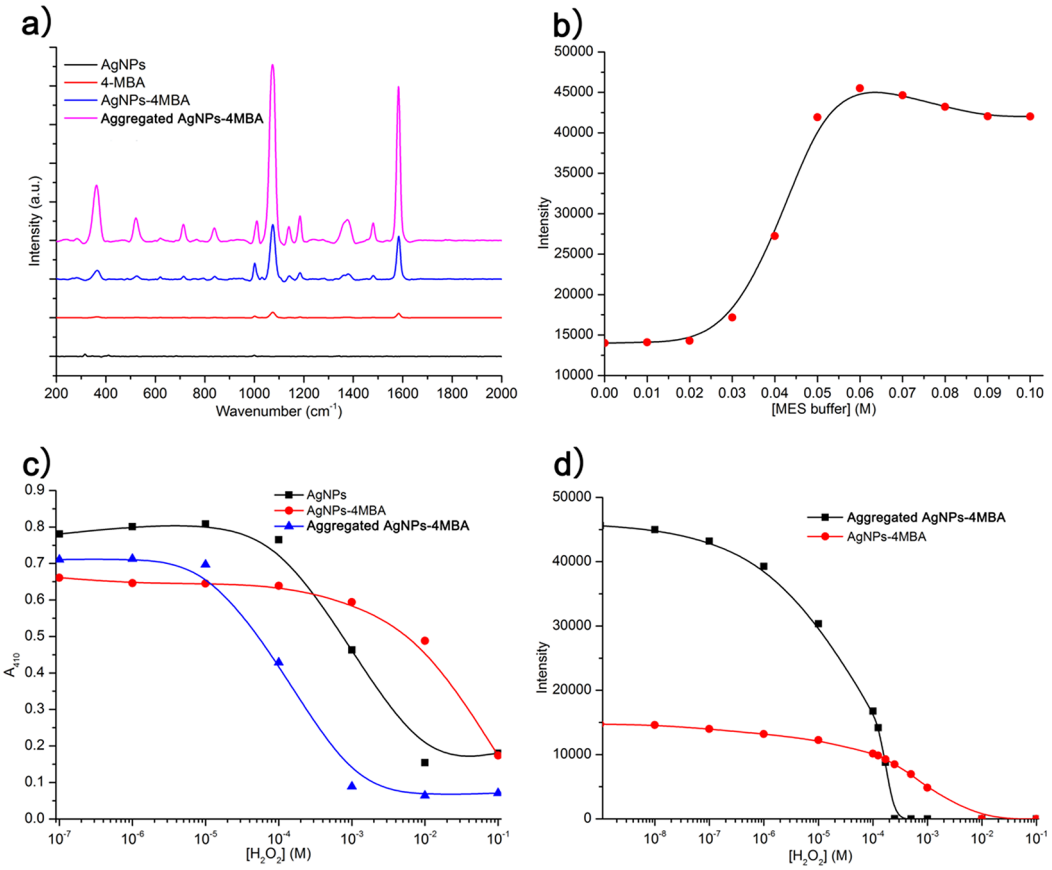

Figure 3. (a) Raman spectra of AgNPs, 4-MBA, and AgNPs−4MBA in ultrapure water and aggregated AgNPs−4MBA in MES buffer. The characteristic peak of the Raman shift for 4-MBA is 1077 cm^{-1}. (b) Raman signal intensity at 1077 cm^{-1} of AgNPs−4MBA dissolved in a concentration gradient of MES buffer. (c) The absorbance at 410 nm after introducing various concentrations of hydrogen peroxide into AgNPs, AgNPs−4MBA, and aggregated AgNPs−4MBA. (d) Raman signal intensity at 1077 cm^{-1} after introducing various concentrations of hydrogen peroxide into AgNPs−4MBA and aggregated AgNPs−4MBA.

Zetaszier Nano ZS, Rigaku D/max-rB analysis instrument, and Thermo Fisher inductively coupled plasma mass spectrometer, respectively.

Preparation of Substrate Reaction Solution (Solution A and Solution B). Solution A is 200 μM hydrogen peroxide. Solution B is aggregated AgNPs−4MBA. Silver colloid was prepared according to Lee and Meisel's method.[31] Then 90 mg of silver nitrate was dissolved in 500 mL of hyperpure water and the solution was heated to boiling. Following this procedure, 10 mL of a 1% trisodium citrate aqueous solution was added dropwise to the boiling silver nitrate solution and vigorously stirred. The mixed solution was boiled for an additional 30 min and produced a stable green-gray Ag colloid. AgNPs−4MBA were prepared as follows:[32] 10 μL of 1 mM 4-MBA was dissolved in ethanol, mixed with 10 mL of Ag colloid; the solution was consistently stirred for 24 h at room temperature, centrifuged at 6000 rpm for 10 min at 4 °C, and the supernatant was discarded. The resulting pellet (AgNPs−4MBA) was suspended in 10 mL of hyperpure water. Prepared AgNPs−4MBA was dissolved in MES buffer (2-(*N*-morpholino)ethanesulfonic acid, pH 6.4) to form solution B.

Preparation of the Detection Probe. The detection probe (detection antibody linked with catalase through gold nanoparticles) was prepared according to the previous reported method.[17,33] Briefly, 100 mL of 0.02% gold chloride trihydrate solution in superpurified water was heated to boiling, and then 4.0 mL of 1% sodium citrate solution was added quickly into the solution under stirring over a period of 20 min, then were obtained 20 nm gold nanoparticles. The pH of the gold nanoparticles solution for detection antibody and catalase conjugation was adjusted to 8.3 with 0.15 mol/L potassium carbonate. The stock solutions of detection antibody (1 mg/mL) and catalase (1 mg/mL) were mixed at the ratios of 1:4. Then the mixture solution (0.1 mL) was added into 10 mL of gold nanoparticles solution. The solution was agitated for 20 min and stood for 2 h at room temperature without mixing. The probes were purified by centrifugation at 10 100*g* for 30 min to remove unconjugated protein molecules and then resuspended in 10 mL of PBS solution (containing 1% BSA).

Sandwich Assay for PSA. The 96-well polystyrene plates (JET BIOFIL) were coated with mouse monoclonal anti-PSA (100 μL, Abcam), diluted by 1:300 in PBS at 4 °C overnight. After washing the plates three times with wash buffer (1% Tween-20 in PBS), the plates were blocked with blocking buffer (1 mg/mL BSA in PBS) for 1 h at 37 °C. Subsequently, the plates were washed three times with wash buffer, and PSA (100 μL, Sigma) was added to the desired final concentration by dilution with PBS. After being incubated for 1 h at 37 °C, the plates were washed three times with wash buffer, and the detection probe was added and incubated for 1 h at 37 °C. After washing the plates three times with wash buffer, twice with PBS, and once with deionized ultrapure water, solution A (100 μL) was added to each well of the plate. After 30 min,

DOI: 10.1021/acs.analchem.5b01011
Anal. Chem. XXXX, XXX, XXX−XXX

freshly prepared solution B (100 μL) was added to each well. After 40 min, each well was detected by an Advantage 785 Raman spectrometer (25 mW, 785 nm, 20 s) to obtain the Raman signal intensity.

Competitive Assay for Rac. The 96-well polystyrene plates (JET BIOFIL) were coated with the antigen (100 μL, Rac−BSA synthesized by our lab) diluted to 100 μg/mL in bicarbonate buffer (100 mM, pH 9.6) at 4 °C overnight. After washing the plates three times with wash buffer (1% Tween-20 in PBS), the plates were blocked with blocking buffer (1 mg/mL BSA in PBS) for 1 h at 37 °C. Subsequently, the plates were washed three times with wash buffer, and Rac (50 μL, Sigma) was added to the desired final concentration by dilution in PBS. Then, mouse monoclonal anti-Rac (50 μL, prepared by our lab) was added. After being incubated for 1 h at 37 °C, the plates were washed three times with wash buffer, and the detection probe was added and incubated for 1 h at 37 °C. After washing the plates three times with wash buffer, twice with PBS, and once with deionized ultrapure water, solution A (100 μL) was added to each well of the plate. After 30 min, freshly prepared solution B (100 μL) was added to each well. After 40 min, each well was detected by an Advantage 785 Raman spectrometer (25 mW, 785 nm, 20 s) to obtain the Raman signal intensity.

RESULTS AND DISCUSSION

Aggregation of AgNPs−4MBA. In this novel signal system, we choose MES buffer (pH = 6.4) as the basic buffer of substrate solution B. First, salt ions in the MES buffer can lead to the aggregation of AgNPs.[34] Second, MES buffer is acidic, which can improve the capability of hydrogen peroxide to oxidize.[35] To test the aggregation of AgNPs−4MBA, we first achieved a coupling between the Raman reporter molecule 4-MBA (with a characteristic peak of the Raman shift at 1077 cm^{-1}) and AgNPs by forming a Ag−S bond.[28] The ζ-potential (Supporting Information Figure S1) and Raman spectrum (Figure 3a) of naked and modified AgNPs solutions were obtained. The difference in the ζ-potential and Raman signal between naked and modified AgNPs illustrates the successful coupling between 4-MBA and AgNPs (AgNPs−4MBA). Subsequently, AgNPs−4MBA were dissolved in different concentration of MES buffer to form aggregated AgNPs−4MBA. DLS results indicated that the size of AgNPs−4MBA (Supporting Information Figure S2) increased with increasing concentrations of MES buffer. Additionally, TEM images of AgNPs−4MBA dissolved in ultrapure water, 20 mM MES buffer, and 60 mM MES buffer (Supporting Information Figure S3) show that aggregation of AgNPs−4MBA occurred in the MES buffer. Figure 3a also clearly shows that AgNPs−4MBA dissolved in 60 mM MES buffer can greatly enhance the SERS effect. To determine whether the SERS effect was significantly enhanced by aggregated AgNPs−4MBA, the Raman signals of AgNPs−4MBA dissolved in different concentrations of MES buffer were determined (Figure 3b). The experimental results indicated that this simple method can significantly enhance the SERS effect but also indicated that the SERS intensity begins to decrease with MES buffer concentrations above 60 mM. It may be due to the fact that, as we increase the concentration of MES buffer, aggregates or cluster size increases. Since it is known that a small cluster is better for hot spot formation, increasing cluster size may decrease the number of hot spots and thus decrease the SERS intensity. The same phenomenon also occurred in another study;[36] however, for our purposes, we need only to choose an optimal concentration of MES buffer to significantly enhance the SERS effect. We probed the optimal concentration of MES buffer with increasing hydrogen peroxide concentration (Supporting Information Figure S4). We found that the signal intensity is the highest when the concentration of MES buffer reaches 60 mM. Meanwhile, the hydrogen peroxide-dependent signal reduction is sharp in this concentration. So we think 60 mM MES buffer is the reasonable concentration. In conclusion, we choose 60 mM MES buffer to form aggregated AgNPs−4MBA as reaction solution B to finish our experiments.

Oxidation of AgNPs−4MBA. Hydrogen peroxide is a powerful oxidant that is strongly dependent on the acidity of the solution.[35] Under acidic conditions:

$$H_2O_2 + 2H^+ + 2e^- \rightarrow 2H_2O \qquad E^0 = 1.763\ V$$

Under alkaline conditions:

$$H_2O_2 + 2e^- \rightarrow 2OH^- \qquad E^0 = 0.867\ V$$

The redox potential for AgNPs is given as follows:

$$Ag^+ + e^- \rightarrow Ag \qquad E^0 = 0.7996\ V$$

Hydrogen peroxide has a standard potential of 1.763 V in acidic solutions and 0.867 V in alkaline solutions, both of which are higher than the potential of Ag^+/Ag (0.7996 V), suggesting that hydrogen peroxide can be used as an effective oxidizing agent to dissolve metallic silver.[37] We added a rang of hydrogen peroxide concentrations to the AgNPs solution to determine whether this oxidation occurred (Supporting Information Figure S5a). The absorbance decreased when increasing hydrogen peroxide concentration, and the yellow color of the solution became transparent. Furthermore, it is possible to monitor the degradation of AgNPs by measuring the absorbance at 410 nm (Figure 3c). The change of absorbance at 410 nm is due to the catalytic decomposition of hydrogen peroxide, which induces the degradation of AgNPs. X-ray diffraction analysis was conducted to further confirm this oxidation mechanism. The intensity of the peaks at 39° relative to the face-centered cubic crystalline silver varied based on the concentration of hydrogen peroxide. Specifically, the AgNP colloid without hydrogen peroxide exhibited a strong intensity peak at 39°, the AgNP colloid with 10^{-5} M hydrogen peroxide exhibited a weaker peak intensity, and the AgNP colloid with 10^{-2} M hydrogen peroxide exhibited no peak (Supporting Information Figure S6). The absence of all diffraction peaks characteristic of silver indicated that a more concentrated hydrogen peroxide solution induced the complete decomposition of NPs.[38] To determine whether hydrogen peroxide could also oxidize AgNPs−4MBA, we performed the same procedures as above using AgNPs−4MBA instead of AgNPs. The results of the absorbance assay (Supporting Information Figure S5b) were the same when using AgNPs−4MBA. It is also possible to monitor the degradation of AgNPs−4MBA by measuring the absorbance at 410 nm (Figure 3c). The results of this assay indicate that hydrogen peroxide is capable of oxidizing AgNPs−4MBA, but in a different manner than AgNPs. The absorbance at 410 nm of AgNPs−4MBA exhibits a smaller change than that of AgNPs at the same concentration of hydrogen peroxide. These results might indicate that 4-MBA could effectively protect the AgNPs from oxidation. The protective ability of 4-MBA makes it more difficult to oxidize AgNPs−4MBA, leading to a decrease in detection sensitivity.[39]

DOI: 10.1021/acs.analchem.5b01011
Anal. Chem. XXXX, XXX, XXX−XXX

To verify the functionality of the novel signal detection system, we measured the Raman spectrum for AgNPs−4MBA with different concentrations of hydrogen peroxide (Figure 3d) and found that the characteristic peak at 1077 cm^{-1} disappeared when the concentration of hydrogen peroxide reached a high level. This finding indicates that the novel system that we designed is feasible but may not provide adequate sensitivity.

Fortunately, the MES buffer that we used in this novel system to properly aggregate nanoparticles exhibited acidity, so it may be possible to increase the sensitivity, as hydrogen peroxide is easier to oxidize AgNPs under acidic conditions. To confirm that the aggregated AgNPs−4MBA can be easier oxidized by hydrogen peroxide in MES buffer, we monitored the absorbance of aggregated AgNPs−4MBA solution at 410 nm with different concentrations of hydrogen peroxide (Figure 3c and Supporting Information Figure S7a) and found that the MES buffer is capable of enhancing the oxidation of hydrogen peroxide, facilitating the oxidation of AgNPs−4MBA. Finally, to demonstrate the functionality of the novel ELISA signal generation system, we used Raman spectroscopy to assess aggregated AgNPs−4MBA solution with different concentrations of hydrogen peroxide (Figure 3d). The Raman signal at 1077 cm^{-1} disappeared when the concentration reached a high level, and the concentration of hydrogen peroxide required to eliminate the Raman signal is less than that required without MES buffer. After reacting with hydrogen peroxide, the supernatant of the reacted solutions was measured by ICP (Supporting Information Figure S7b), and the ICP result showed that a high concentration of Ag^+ was detected in reacted solution, which indicated the AgNPs of aggregated AgNPs−4MBA were oxidized to Ag^+. In conclusion, the proposed method is feasible for hydrogen peroxide-related detection. A change of 20 μM hydrogen peroxide still leads to ∼5000 difference value of Raman signal intensity, as shown in Figure 3d. We choose 200 μM hydrogen peroxide as reaction solution A to finish our experiments.

Sandwich AAN−SERS−ELISA for PSA Detection and Analysis of Clinical Samples. PSA has been recognized as a valuable biomarker for cancer recurrence in patients who have undergone radical prostatectomy.[40] For these patients, it is vital to detect small concentrations of PSA at the earliest possible stage to improve survival rates. PSA is a large protein biomarker, and a model molecule to be detected by our sandwich AAN−SERS−ELISA. Figure 4a shows the results for the detection of PSA with AAN−SERS−ELISA when these proteins were spiked into whole serum. Control experiments performed by spiking an unrelated globular protein, BSA, in the serum led to the weakest SERS effect because the antibodies could not specifically recognize this protein. In the calibration curves, the detection limit for PSA, defined as the lowest assayed concentration that yielded an obvious signal, is 10^{-9} ng/mL (Figure 4b). The unusually low detection limit probably is attributed to the high SERS effects of aggregated AgNPs and the high efficiency of the catalase (40 000−60 000 units/mg, the enzymatic activity of horse radish peroxidase is only several hundred units per milligram) for fine-tuning the concentration of hydrogen peroxide, which is the driving force in the dissolution of aggregated AgNPs−4MBA.

The robustness of the analytical procedure against possible interferences found in real samples should also be evaluated. To study the impact of real matrixes on the detection of PSA, sera from 20 donors were assayed with the AAN−SERS−ELISA. These donors were suspected prostatic cancer patients whose

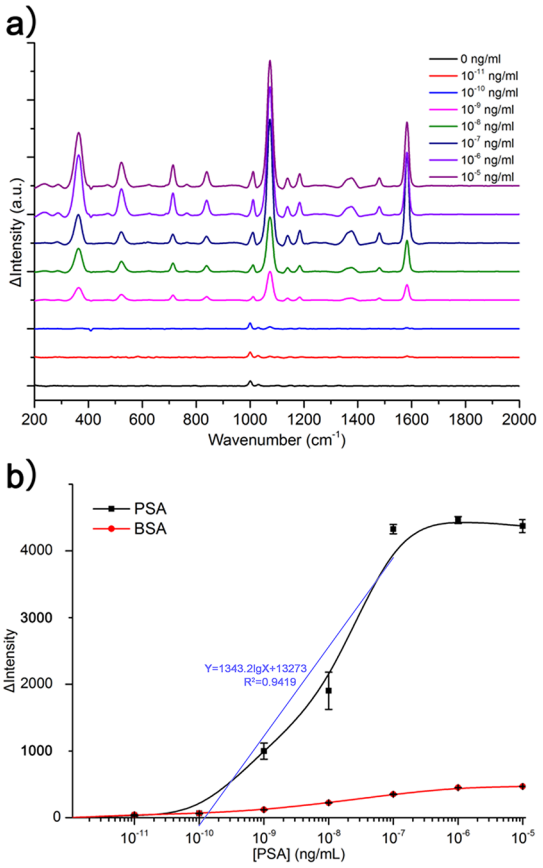

Figure 4. (a) Raman spectra of different PSA concentrations determined by AAN−SERS−ELISA. (b) PSA concentration-dependent Raman intensity of 1077 cm^{-1} peak. (ΔIntensity is expressed as the Raman intensity of 1077 cm^{-1} peak of sample minus that of the blank.) Black curves were obtained by spiking PSA into bovine serum. Red curves were obtained by spiking unrelated protein BSA. Error bars indicate the standard deviation of three independent measurements.

PSA levels were determined using time-resolved fluorescent immunoassays (TRFIAs). All sera were diluted 10^9-fold with PBS and then detected by our AAN−SERS−ELISA. The AAN−SERS−ELISA results of the samples from suspected prostatic cancer patients are in accordance with the results of TRFIAs shown in Figure 5. The results from the two methods correlated well, which indicates that the AAN−SERS−ELISA can be used to identify low concentrations of cancer protein biomarkers in clinical samples.

Competitive AAN−SERS−ELISA for Rac Detection. To test whether the novel signal generation system works in competitive ELISA, Rac was used as a model analyte. Rac is a phenol amine β adrenal stimulant that can enhance athletes' muscles and improve performance. But it is harmful to users' health, so it has been listed as a forbidden stimulant drug by the international Olympic committee. Rac is a small molecule, so it is usually detected by competitive immunoassays. Figure 6a shows the results for the detection of Rac with AAN−SERS−ELISA when Rac was spiked into urine. Control experiments performed by spiking an unrelated analyte, clenbuterol. In the calibration curves, the detection limit for Rac, defined as the lowest assayed concentration that yielded a weaker signal, was 10^{-6} ng/mL (Figure 6b). The result indicated that this ultrasensitive detection system also works in competitive

DOI: 10.1021/acs.analchem.5b01011
Anal. Chem. XXXX, XXX, XXX−XXX

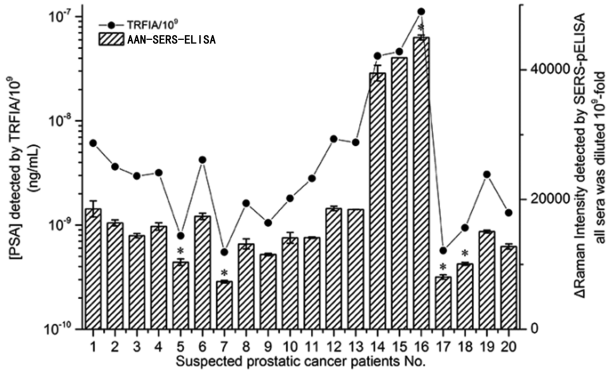

Figure 5. Detection of PSA in human sera using the AAN–SERS–ELISA and comparison with the TRFIA. PSA samples collected from sera of 20 suspected prostate cancer patients were used to evaluate the detection performance of the AAN–SERS–ELISA. Nos. 5, 7, 16, 17, and 18, indicated by an asterisk (*), are outside the linear range. Error bars indicate the standard deviation of three independent measurements.

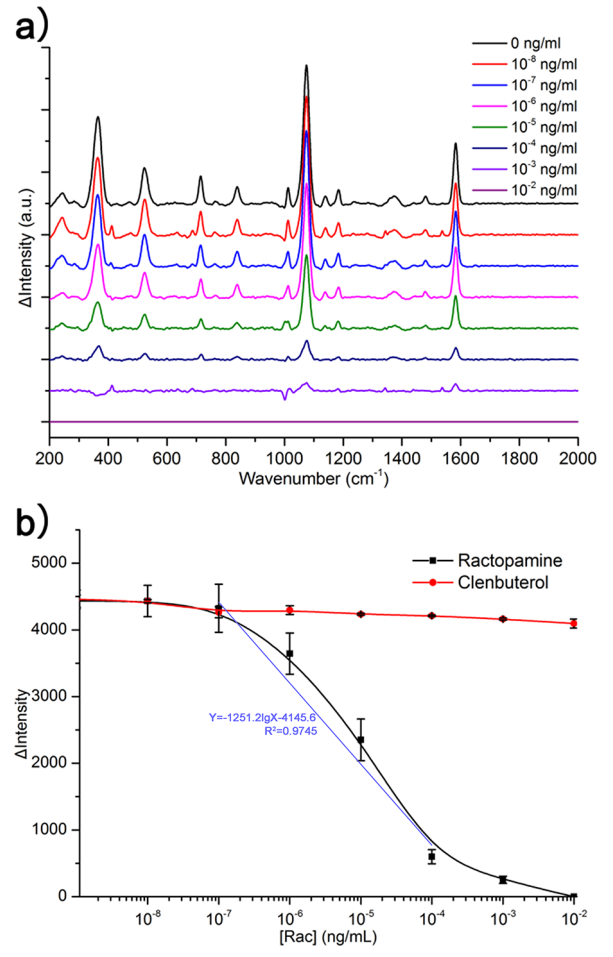

Figure 6. (a) Raman spectra of different Rac concentrations determined by AAN–SERS–ELISA. (b) Rac concentration-dependent Raman intensity of 1077 cm^{-1} peak. (ΔIntensity is expressed as the Raman intensity of 1077 cm^{-1} peak of sample minus that of the blank.) Black curves were obtained by spiking Rac into urine. Red curves were obtained by spiking unrelated analyte CL. Error bars indicate the standard deviation of three independent measurements.

AAN–SERS–ELISA and can detect ultralow concentrations of small molecular analytes.

CONCLUSIONS

We used aggregated Raman tag-labeled AgNPs for ultrasensitive detection of proteins and small molecules by combining an additional enhanced SERS signal generation system with an ELISA. The ultrasensitive detection of PSA could be useful for cancer recurrence prognosis for patients who have undergone radical prostatectomy. The ultrasensitive detection of Rac could be useful for justice in a sporting match. For regular detection, the conventional ELISA, with relatively low sensitivity, remains simple and convenient. The AAN–SERS–ELISA uses multistage signal amplification to obtain higher Raman signal, including the additional SERS effect of aggregated AgNPs and the high enzymatic activity of catalase. These strategies enable the novel AAN–SERS–ELISA to achieve ultrasensitive detection by using similar operational processes and little longer durations to conventional ELISAs. This ultrasensitive method allows the practical samples to be repeatedly diluted, thus reducing interference from other substances. Moreover, many other biomarkers or analytes need to be detected in ultralow concentration.

Although the sensitivity of this novel strategy is ultrahigh, some disadvantages still should be overcome in the further study. The conventional Raman spectrometer is a little expensive and inconvenient; as more and more low-cost portable Raman spectrometers are manufactured, these portable devices can be used with AAN–SERS–ELISAs to reduce cost.[41] Moreover, the efficiency of the catalase is high but the stability of catalase should be further improved. Because the signal generation system was related to immunoassays through hydrogen peroxide, the enzymes which can produce or decompose H_2O_2, such as glucose oxidase (catalysis of glucose to produce hydrogen peroxide) and peroxidase, also can be used in this system.

In conclusion, we have developed a novel signal generation system of ELISA and achieved ultrasensitive detection of both small and large molecules.

ASSOCIATED CONTENT

Supporting Information

Operation details of TRFIAs, plots of size (DLS) and ζ-potential measurements, TEM images, absorption spectrum, and X-ray diffraction pattern. The Supporting Information is available free of charge on the ACS Publications website at DOI: 10.1021/acs.analchem.5b01011.

AUTHOR INFORMATION

Corresponding Authors

*E-mail: zhluocn@gmail.com.

*E-mail: tyjaq7926@163.com.

Author Contributions

‖J.L., H.L., and C.H. contributed equally to this work. The manuscript was written through contributions of all authors. All authors have given approval to the final version of the manuscript.

Notes

The authors declare no competing financial interest.

ACKNOWLEDGMENTS

This work was supported by the Ministry of Education to Study the Scientific Research Foundation of China (47), the Technology Research Program of Guangdong Province (2013B010404027), and the National Science Foundation of

DOI: 10.1021/acs.analchem.5b01011
Anal. Chem. XXXX, XXX, XXX–XXX

China (11204105). This manuscript has been edited and proofread by NPG Language Editing.

REFERENCES

(1) Fu, Q.; Tang, Y.; Shi, C.; Zhang, X.; Xiang, J.; Liu, X. *Biosens. Bioelectron.* **2013**, *49*, 399−402.
(2) Rissin, D. M.; Kan, C. W.; Campbell, T. G.; Howes, S. C.; Fournier, D. R.; Song, L.; Piech, T.; Patel, P. P.; Chang, L.; Rivnak, A. J. *Nat. Biotechnol.* **2010**, *28*, 595−599.
(3) Miranda, O. R.; Chen, H.-T.; You, C.-C.; Mortenson, D. E.; Yang, X.-C.; Bunz, U. H.; Rotello, V. M. *J. Am. Chem. Soc.* **2010**, *132*, 5285−5289.
(4) Giljohann, D. A.; Mirkin, C. A. *Nature* **2009**, *462*, 461−464.
(5) Yolken, R. H.; Barbour, B.; Wyatt, R. G.; Kalica, A. R.; Kapikian, A. Z.; Chanock, R. M. *Science* **1978**, *201*, 259−262.
(6) Wegner, G. J.; Lee, H. J.; Corn, R. M. *Anal. Chem.* **2002**, *74*, 5161−5168.
(7) Hayes, F. J.; Halsall, H. B.; Heineman, W. R. *Anal. Chem.* **1994**, *66*, 1860−1865.
(8) Landry, J.; Zhu, X.; Gregg, J. *Opt. Lett.* **2004**, *29*, 581−583.
(9) Wang, Y.; Salehi, M.; Schütz, M.; Schlücker, S. *Chem. Commun.* **2014**, *50*, 2711−2714.
(10) Li, T.; Guo, L.; Wang, Z. *Biosens. Bioelectron.* **2008**, *23*, 1125−1130.
(11) Chen, Z.; Tabakman, S. M.; Goodwin, A. P.; Kattah, M. G.; Daranciang, D.; Wang, X.; Zhang, G.; Li, X.; Liu, Z.; Utz, P. J. *Nat. Biotechnol.* **2008**, *26*, 1285−1292.
(12) Wu, G.; Datar, R. H.; Hansen, K. M.; Thundat, T.; Cote, R. J.; Majumdar, A. *Nat. Biotechnol.* **2001**, *19*, 856−860.
(13) Zheng, G.; Patolsky, F.; Cui, Y.; Wang, W. U.; Lieber, C. M. *Nat. Biotechnol.* **2005**, *23*, 1294−1301.
(14) Nam, J.-M.; Thaxton, C. S.; Mirkin, C. A. *Science* **2003**, *301*, 1884−1886.
(15) Kong, J.; Franklin, N. R.; Zhou, C.; Chapline, M. G.; Peng, S.; Cho, K.; Dai, H. *Science* **2000**, *287*, 622−625.
(16) Lin, H.; Liu, Y.; Huo, J.; Zhang, A.; Pan, Y.; Bai, H.; Jiao, Z.; Fang, T.; Wang, X.; Cai, Y. *Anal. Chem.* **2013**, *85*, 6228−6232.
(17) Zou, J.; Tang, Y.; Zhai, Y.; Zhong, H.; Song, J. *Anal. Methods* **2013**, *5*, 2720−2726.
(18) Farrell, C. D.; Rowell, F. J.; Cumming, R. H. *Anal. Proc. incl. Anal. Commun.* **1995**, *32*, 205−206.
(19) Roda, A.; Guardigli, M.; Michelini, E.; Mirasoli, M.; Pasini, P. *Anal. Chem.* **2003**, *75*, 462A−470A.
(20) Cao, Y. C.; Jin, R.; Nam, J.-M.; Thaxton, C. S.; Mirkin, C. A. *J. Am. Chem. Soc.* **2003**, *125*, 14676−14677.
(21) Liu, D.; Yang, J.; Wang, H.-F.; Wang, Z.; Huang, X.; Wang, Z.; Niu, G.; Hight Walker, A.; Chen, X. *Anal. Chem.* **2014**, *86*, 5800−5806.
(22) Liu, D.; Wang, Z.; Jin, A.; Huang, X.; Sun, X.; Wang, F.; Yan, Q.; Ge, S.; Xia, N.; Niu, G. *Angew. Chem., Int. Ed.* **2013**, *52*, 14065−14069.
(23) de la Rica, R.; Velders, A. H. *Small* **2011**, *7*, 66−69.
(24) de la Rica, R.; Stevens, M. M. *Nat. Protoc.* **2013**, *8*, 1759−1764.
(25) Zhang, Y.; Guo, Y.; Xianyu, Y.; Chen, W.; Zhao, Y.; Jiang, X. *Adv. Mater.* **2013**, *25*, 3802−3819.
(26) de La Rica, R.; Stevens, M. M. *Nat. Nanotechnol.* **2012**, *7*, 821−824.
(27) Rodríguez-Lorenzo, L.; de La Rica, R.; Álvarez-Puebla, R. A.; Liz-Marzán, L. M.; Stevens, M. M. *Nat. Mater.* **2012**, *11*, 604−607.
(28) Wu, Z.; Liu, Y.; Zhou, X.; Shen, A.; Hu, J. *Biosens. Bioelectron.* **2013**, *44*, 10−15.
(29) Feuz, L.; Jonsson, M. P.; Höök, F. *Nano Lett.* **2012**, *12*, 873−879.
(30) Pieczonka, N. P.; Aroca, R. F. *ChemPhysChem* **2005**, *6*, 2473−2484.
(31) Lee, P.; Meisel, D. *J. Phys. Chem.* **1982**, *86*, 3391−3395.
(32) Liang, J.; Liu, H.; Lan, C.; Fu, Q.; Huang, C.; Luo, Z.; Jiang, T.; Tang, Y. *Nanotechnology* **2014**, *25*, 495501.
(33) Li, Y. S.; Zhou, Y.; Meng, X. Y.; Zhang, Y. Y.; Liu, J. Q.; Zhang, Y.; Wang, N. N.; Hu, P.; Lu, S. Y.; Ren, H. L.; Liu, Z. S. *Biosens Bioelectron* **2014**, *61*, 241−244.
(34) Pamies, R.; Cifre, J. G. H.; Espín, V. F.; Collado-González, M.; Baños, F. G. D.; de la Torre, J. G. *J. Nanopart. Res.* **2014**, *16*, 1−11.
(35) Ho, C.-M.; Yau, S. K.-W.; Lok, C.-N.; So, M.-H.; Che, C.-M. *Chem.-Asian J.* **2010**, *5*, 285.
(36) Dasary, S. S.; Singh, A. K.; Senapati, D.; Yu, H.; Ray, P. C. *J. Am. Chem. Soc.* **2009**, *131*, 13806−13812.
(37) Yang, X.; Yu, Y.; Gao, Z. *ACS Nano* **2014**, *8*, 4902−4907.
(38) Clemenson, S.; David, L.; Espuche, E. *J. Polym. Sci., Part A: Polym. Chem.* **2007**, *45*, 2657−2672.
(39) Tan, K.; Yang, G.; Chen, H.; Shen, P.; Huang, Y.; Xia, Y. *Biosens. Bioelectron.* **2014**, *59*, 227−232.
(40) Thaxton, C. S.; Elghanian, R.; Thomas, A. D.; Stoeva, S. I.; Lee, J.-S.; Smith, N. D.; Schaeffer, A. J.; Klocker, H.; Horninger, W.; Bartsch, G. *Proc. Natl. Acad. Sci. U. S. A.* **2009**, *106*, 18437−18442.
(41) Ayas, S.; Cupallari, A.; Ekiz, O. O.; Kaya, Y.; Dana, A. *ACS Photonics* **2013**, *1*, 17−26.

DOI: 10.1021/acs.analchem.5b01011
Anal. Chem. XXXX, XXX, XXX−XXX